Effect of losses on the performance of an SU(1,1) interferometer

A. M. Marino,[1] N. V. Corzo Trejo,[1,2] and P. D. Lett[1,*]

[1]*Quantum Measurement Division, National Institute of Standards and Technology, and Joint Quantum Institute, NIST and the University of Maryland, Gaithersburg, Maryland 20899, USA*

[2]*Departamento de Física, CINVESTAV-IPN, México D.F., 07360 México*

(Received 1 June 2012; published 24 August 2012)

We study the effect of losses on the phase sensitivity of the SU(1,1) interferometer for different configurations. We find that this type of interferometer is robust against losses that result from an inefficient detection system. This type of loss only introduces an overall prefactor to the sensitivity but does not change the $1/n$ scaling, where n is the average number of particles inside the interferometer, characteristic of the Heisenberg limit. In addition, we show that under some conditions the SU(1,1) interferometer with coherent state inputs is also robust against internal losses. These results show that the SU(1,1) interferometer is a viable candidate for experimentally reaching the Heisenberg limit with current technology. Possible implementations of this interferometer using four-wave mixing in atomic vapors or an atom interferometer in a spinor Bose-Einstein condensate are compared.

DOI: 10.1103/PhysRevA.86.023844 PACS number(s): 42.50.St, 07.60.Ly, 42.65.Yj

I. INTRODUCTION

The field of quantum metrology [1] explores the possibility of using quantum resources to enhance the sensitivity of measurements beyond what can be achieved with only classical resources. In particular, interferometers have been the device of choice to pursue this goal. These devices offer an invaluable tool in the field of precision measurement because they make it possible to estimate very small phase changes. With the use of only classical resources, the phase sensitivity of an interferometer is limited by shot noise and is bounded by $1/\sqrt{n}$, where n is the average number of particles inside the interferometer. This limit is known as the classical limit, the shot noise limit, or the standard quantum limit (SQL). The use of quantum resources offers the possibility of beating the SQL and reaching the Heisenberg limit (HL), characterized by a phase sensitivity that scales as $1/n$. The possibility of beating the classical limit was first realized by Caves [2] and has been an intense field of research since then.

A number of different interferometer configurations have been proposed to beat the classical limit. The most studied configuration has been the Mach-Zehnder interferometer. For this interferometer a number of theoretical proposals have shown that it is possible to go below the SQL using nonclassical states of light, such as squeezed states [2,3], Fock states [4], two-mode squeezed states [5], NOON states [6], etc. The main constraint in implementing these proposals has been the sensitivity of this interferometer to losses, both internal and external. It has been shown, in general, that the effect of losses can be detrimental in beating the SQL [7–12]. Only recently has it been shown that the use of more complicated detection strategies based on Bayesian parameter estimation makes it possible to beat the SQL even in the presence of losses for the Mach-Zehnder interferometer [13–15].

Another possibility for beating the SQL is to use an interferometer in which the mixing of the optical beams is done through a nonlinear transformation, such as the SU(1,1) interferometer (see Fig. 1). This type of interferometer is configured like a Mach-Zehnder interferometer except that the beam splitters are replaced with parametric processes that can generate correlated pairs. It has been shown that this type of interferometer can reach the HL in the absence of losses [16]. Recently, theoretical analysis has shown that having coherent states as inputs into the interferometer can provide an improvement in the sensitivity [17]. In addition, an experimental implementation of this interferometer in the classical domain has been recently realized [18]. The possibility of extending such an implementation to the quantum domain and beat the SQL requires an analysis of the effect of losses. Such an analysis has only recently been done [19], but it was limited to the study of the impact of losses on the signal-to-noise ratio for homodyne detection of one of the outputs of the interferometer. A full analysis of the effect of losses on the phase sensitivity (or uncertainty in the phase estimate) that can be achieved with the SU(1,1) interferometer is still missing. In this paper we take a closer look at this problem when direct detection of both outputs is considered and analyze both the effect of internal losses and losses after the interferometer (external losses) that would model the use of inefficient detectors. We show that even though external losses reduce the sensitivity of the interferometer, they do not prevent it from beating the SQL and, in fact, do not change the scaling characteristic of the HL. In addition, we show that in general the phase sensitivity of the SU(1,1) interferometer is extremely sensitive to internal losses, making it impossible to reach the HL and typically even perform below the SQL. We show, however, that this interferometer can be made robust against internal losses under the condition that both input ports are seeded with coherent states. In this configuration internal losses still degrade the phase sensitivity; however, it is still possible to beat the SQL even with a significant amount of loss.

Finally, we discuss two possible physical implementations of the SU(1,1) interferometer. The first would use a four-wave mixing (4WM) interaction in Rb vapor and closely mirrors the original proposals for this sort of interferometer [16]. We discuss real-world limitations on this particular technology,

*paul.lett@nist.gov

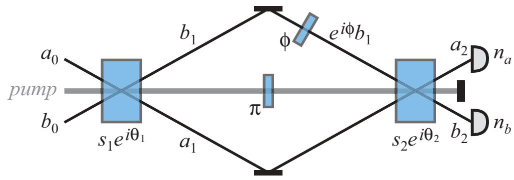

FIG. 1. (Color online) Schematic drawing of an ideal SU(1,1) interferometer. An SU(1,1) interferometer is similar to a Mach-Zehnder interferometer except that the input and output beam splitters are replaced by parametric processes. The interferometer is typically studied in a balanced configuration, in which the parametric process in the second region is set to undo the interaction in the first region.

including losses and mode-matching, that would likely be encountered. We also discuss an atom interferometer version of this idea, implemented with spinor Bose-Einstein condensates confined in a relatively tight laser dipole trap, which could avoid many of the concerns brought up in the context of the optical 4WM version.

II. IDEAL SU(1,1) INTERFEROMETER

We start with a study of the ideal lossless SU(1,1) optical interferometer. In its basic configuration this type of interferometer is like a Mach-Zehnder interferometer with the beam splitters replaced by parametric processes, as shown in Fig. 1, such as parametric down-conversion or 4WM. The parametric process requires the use of one or two strong pump beams (depending on the process used) in addition to two beams, labeled a and b in Fig. 1, that travel the two paths of the interferometer. This process is characterized by two parameters: s, which is proportional to the strength of the process, and θ, which describes the phase shift introduced by the process. In the parametric process photons are transferred between the pump beam and beams a and b with the direction of the transfer dictated by the phases of the fields involved in the process. Thus, it is possible to have amplification or deamplification of beams a and b. Since energy can be transferred from the pump to beams a and b, this interferometer can be used without any input fields into paths a and b.

The SU(1,1) interferometer is typically studied in a balanced configuration in which the second parametric process is set to "undo" what the first parametric process did. In this configuration the first parametric process generates entangled pairs of photons, with one photon from each pair going into each of the arms of the interferometer. Then, the second parametric process undoes what the first one did by transferring the pair of photons back to the pump beam. This is accomplished by introducing a π phase shift between the pump (or $\pi/2$ for 4WM where two pump photons are needed) and beams a and b after the first parametric process. If there is no phase difference between the two paths of the interferometer ($\phi = 0$) then the output beams of the interferometer are equal to the input beams. How well this is accomplished depends on the efficiency of the second process, that is, how many of the generated photons are transferred back to the pump, which depends on the relative phases of the pump and beams a and b. Thus, any change in the relative phase ϕ between the arms of the interferometer will lead to an incomplete transfer of the entangled photons generated in the first parametric region back to the pump in the second region, and thus to a change in the output optical power and noise properties. These changes can then be used to infer the internal phase difference ϕ.

In general, to study how well an interferometer can be used to estimate the internal phase difference we need a measure of its sensitivity. Such a measure can be obtained through measurements of the optical fields that exit through the two output ports. If one were to measure variable N, consisting of some combination of measurements of the output fields, then the uncertainty in the estimation of the internal phase of the interferometer can be obtained through an error propagation analysis, such that

$$\Delta\phi^2 = \frac{\langle(\Delta\hat{N})^2\rangle}{|\partial\langle\hat{N}\rangle/\partial\phi|^2}. \tag{1}$$

The sensitivity in the measurement is given by the square root of the variance or uncertainty. Note that a smaller value of $\Delta\phi^2$ indicates a reduction in the uncertainty of the estimation and thus an increase in the sensitivity. As can be seen from Eq. (1), the phase sensitivity of the interferometer depends on the noise of the measured variable and on its rate of change with respect to the phase of the interferometer and is dependent on the measurement strategy that is used.

The quantity that is typically measured for an interferometer is the difference in the intensities of the two output ports. For the ideal SU(1,1) interferometer, however, the difference in the intensities of the two output ports is a conserved quantity [20], since photons are always created or eliminated in pairs by the parametric processes, and thus this measure provides no information about ϕ. One can consider instead the total number of photons at the output of the interferometer, that is,

$$\hat{N} = \hat{n}_a + \hat{n}_b = \hat{a}_2^\dagger\hat{a}_2 + \hat{b}_2^\dagger\hat{b}_2, \tag{2}$$

as the variable to be measured to estimate the phase.

The quantities that are needed to calculate $\Delta\phi^2$ can be obtained by using the transformation performed by a parametric process on the field operators for the input modes of the interferometer, $\hat{a}_0$ and $\hat{b}_0$. In this way we find that the two output fields of the SU(1,1) interferometer are given by

$$\hat{a}_2 = a\hat{a}_0 - b\hat{b}_0^\dagger, \tag{3}$$

$$\hat{b}_2 = e^{i\phi}(a\hat{b}_0 - b\hat{a}_0^\dagger), \tag{4}$$

where $a = \cosh s_1 \cosh s_2 + e^{-i\phi}e^{i(\theta_2-\theta_1)}\sinh s_1 \sinh s_2$ and $b = e^{i\theta_1}\sinh s_1 \cosh s_2 + e^{-i\phi}e^{i\theta_2}\cosh s_1 \sinh s_2$, such that $|a|^2 - |b|^2 = 1$. The balanced configuration corresponds to having $s_1 = s_2$ and $\theta_2 = \theta_1 + \pi$, such that with $\phi = 0$ we have $a = 1$ and $b = 0$ and thus $\hat{a}_2 = \hat{a}_0$ and $\hat{b}_2 = \hat{b}_0$.

In general, if the input states are taken to be coherent states with amplitudes $\alpha = |\alpha|e^{i\theta_a}$ and $\beta = |\beta|e^{i\theta_b}$ then we find that

$$\langle\hat{N}\rangle = (|a|^2 + |b|^2)(|\alpha|^2 + |\beta|^2) - 2ab^*\alpha\beta - 2a^*b\alpha^*\beta^* + 2|b|^2, \tag{5}$$

$$\langle(\Delta\hat{N})^2\rangle = (|\alpha|^2 + |\beta|^2)[(|a|^2 + |b|^2)^2 + 4|a|^2|b|^2] - 4(|a|^2 + |b|^2)(ab^*\alpha\beta + a^*b\alpha^*\beta^*) + 4|a|^2|b|^2, \tag{6}$$

$$\frac{\partial\langle\hat{N}\rangle}{\partial\phi} = -4(|\alpha|^2+|\beta|^2+1)\sin(\phi+\theta_1-\theta_2) \times \sinh s_1 \cosh s_1 \sinh s_2 \cosh s_2 + 4|\alpha\beta| \sinh s_2 \cosh s_2[\sin(\phi+\theta_a+\theta_b-\theta_2)\cosh^2 s_1 + \sin(\phi+2\theta_1-\theta_2-\theta_a-\theta_b)\sinh^2 s_1]. \quad (7)$$

The use of these equations gives the most general result for the phase sensitivity of the ideal lossless SU(1,1) interferometer. Throughout the rest of the paper we study the balanced configuration ($s_1 = s_2 \equiv s$ and $\theta_2 = \theta_1 + \pi$) and analyze in more detail different operational regimes as well as the effect of losses. The results obtained can be generalized to the unbalanced case by using the results given above.

We start by analyzing the configuration considered in [16] with no input fields into the interferometer, that is, $|\alpha| = |\beta| = 0$. For the balanced case and for arbitrary ϕ we find that

$$\Delta\phi^2 = \frac{1+2(1-\cos\phi)\sinh^2 s \cosh^2 s}{2(1+\cos\phi)\sinh^2 s \cosh^2 s}. \quad (8)$$

To study the scaling of $\Delta\phi^2$ we need to write Eq. (8) in terms of the total number of photons inside the interferometer. In general, the total number of photons inside the interferometer is determined by the strength of the parametric process s and the phases of the input fields with respect to the phase of the first parametric process θ_1 and can be shown to be of the form

$$n_i = \langle\hat{a}_1^\dagger\hat{a}_1 + \hat{b}_1^\dagger\hat{b}_1\rangle = (|\alpha|^2+|\beta|^2)(\cosh^2 s + \sinh^2 s) - 4|\alpha\beta|\cos\Phi\cosh s\sinh s + 2\sinh^2 s, \quad (9)$$

where $\Phi = \theta_1 - \theta_a - \theta_b$. The first two terms on the right-hand side correspond to contributions from the stimulated parametric process, while the last term results from the spontaneous process. For the particular configuration in which there is no input into the interferometer ($|\alpha| = |\beta| = 0$) the total number of internal photons is given by the spontaneous contribution, that is,

$$n_s = 2\sinh^2 s. \quad (10)$$

With Eqs. (8) and (10) we can now write

$$\Delta\phi^2 = \frac{1}{1+\cos\phi}\left[\frac{2}{n_s(n_s+2)} + (1-\cos\phi)\right]. \quad (11)$$

It is clear from this result that for $\phi = 0$ the uncertainty $\Delta\phi^2$ has a $1/n_s^2$ scaling characteristic of the HL, which corresponds to the result obtained in [16]. In general, however, the performance of the SU(1,1) is phase dependent. As can be seen from Eq. (11) the uncertainty in the phase estimation has two contributions such that for $\phi \neq 0$ the second term will dominate for sufficiently large n_s. Figure 2(a) shows the behavior of $\Delta\phi^2$ as a function of ϕ for a number of different values of n_s. The value of n_s for which the constant term will start to dominate is given by

$$n_s = \sqrt{\frac{3-\cos\phi}{1-\cos\phi}} - 1. \quad (12)$$

After this point the sensitivity becomes independent of n_s, as shown in Fig. 2(b). This result shows that a precise control of ϕ is required in order to reach the HL even in the ideal lossless case.

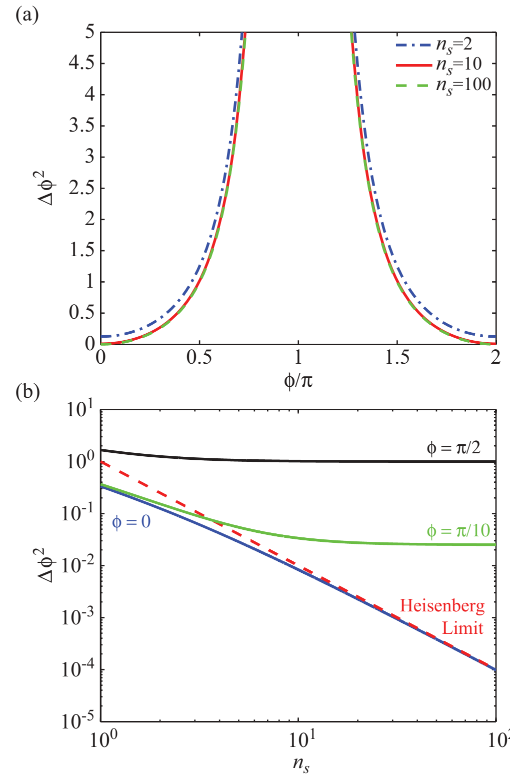

FIG. 2. (Color online) Uncertainty in the phase estimation of the ideal SU(1,1) interferometer with no input fields, Eq. (11), as a function of (a) ϕ for different photon numbers and (b) the number of spontaneous photons inside the interferometer, n_s, for different values of ϕ.

We now look at the configuration in which we have an input in both ports of the interferometer ($|\alpha|,|\beta| \neq 0$). As pointed out in [17], the general expression for this case is rather complicated. We thus consider only the special case where $\phi = 0$ and find that the uncertainty in the phase estimation is given by

$$\Delta\phi^2 = \frac{|\alpha|^2+|\beta|^2}{16|\alpha|^2|\beta|^2\sin^2\Phi\sinh^2 s\cosh^2 s}. \quad (13)$$

As was done in [17], this expression can be written in terms of the internal number of spontaneous photons, such that

$$\Delta\phi^2 = \frac{|\alpha|^2+|\beta|^2}{4|\alpha|^2|\beta|^2 n_s(n_s+2)\sin^2\Phi}, \quad (14)$$

which shows that the uncertainty scales as $1/n_s^2$. Note, however, that since $|\alpha|^2,|\beta|^2 \neq 0$ the total number of photons inside the interferometer, n_i, can be significantly larger than n_s. In general, if we write Eq. (13) in terms of n_i instead of n_s, we find that it has terms that scale as both $1/n_i^2$ and $1/n_i$. However, if we consider the case $\Phi = \pi/2$ and $|\alpha|^2,|\beta|^2 \gg 0$, such that the stimulated photons dominate over the spontaneous ones, then Eq. (13) can be written as

$$\Delta\phi^2 = \frac{|\alpha|^2+|\beta|^2}{4|\alpha|^2|\beta|^2}\frac{1}{[n_i/(|\alpha|^2+|\beta|^2)]^2-1}, \quad (15)$$

where, in this limit, $n_i \simeq (|\alpha|^2 + |\beta|^2)(\cosh^2 s + \sinh^2 s)$. Note that Eq. (15) only contains the number of photons that are internal to the interferometer divided by, or normalized to, the number of photons in the input seed, $n_i/(|\alpha|^2 + |\beta|^2)$. This ratio is always greater than unity and depends only on the strength of the parametric process, s. Thus, except for the prefactor, the scaling of the sensitivity becomes independent of the input coherent amplitudes. It is thus possible to change the sensitivity without changing the power of the seeds by controlling s. As this result shows, in this configuration the HL can be obtained for the SU(1,1) interferometer even when both the stimulated and spontaneous number of photons after the first parametric process are taken into account. As we can see from this result in the limit as $s \to 0$ then $\Delta\phi^2 \to \infty$. This is to be expected since in this limit there is no parametric process and thus no mixing of the input states. As a result, the intensity measurements of the output fields contain no information about the phase.

III. EFFECT OF LOSSES

As has been previously pointed out, the phase sensitivity of an interferometer can be extremely dependent on losses [11,12,21], both in terms of the detection efficiency and internal losses. We now turn to the effect of both of these types of losses on the SU(1,1) interferometer. To simplify the calculations we consider only the case in which both arms of the interferometer have the same internal losses $(1-\eta_1)$ and the detectors for both output beams have the same detection efficiency η_2. After taking into account these losses we find that we can write the rate of change of $\langle\hat{N}\rangle$ with respect to ϕ in terms of the ideal lossless case described in the previous section as

$$\frac{\partial\langle\hat{N}\rangle_l}{\partial\phi} = \eta_1\eta_2\frac{\partial\langle\hat{N}\rangle}{\partial\phi}, \tag{16}$$

where the l subindex indicates that the losses are taken into account. In the same way we find that

$$\begin{aligned}\langle(\Delta\hat{N})^2\rangle_l = {}& \eta_1^2\eta_2^2\langle(\Delta\hat{N})^2\rangle + \eta_1\eta_2[1-\eta_1\eta_2 + 2(1-\eta_1)\eta_2\sinh^2 s]\langle\hat{N}\rangle + 2\eta_1(1-\eta_1)\eta_2^2\sinh s\cosh s\\ &\times[e^{i(\phi-\theta_1)}(a\beta - b\alpha^*)(a\alpha - b\beta^*) - e^{i(\phi-\theta_1)}ab + e^{-i(\phi-\theta_1)}(a^*\beta^* - b^*\alpha)(a^*\alpha^* - b^*\beta) - e^{-i(\phi-\theta_1)}a^*b^*]\\ &+ 2(1-\eta_1)\eta_2\sinh^2 s[1 + (1-\eta_1)\eta_2(\sinh^2 s + \cosh^2 s)].\end{aligned} \tag{17}$$

With these two results we can now calculate the uncertainty in the phase estimation of the interferometer in the presence of losses using Eq. (1).

It has been shown that for the Mach-Zehnder interferometer the losses that result from an inefficient detector can be a significant problem [21,22], thus requiring perfect or almost perfect detectors to obtain a sensitivity below the classical limit. A few schemes such as those based on nonlinear phase shifts [22] and "quantum beam splitters" that can generate NOON states [23] have been shown to be robust against this type of loss mechanism.

We start by looking at the effect of the detection efficiency by making $\eta_1 = 1$ (no internal loss) in the above equations. In this case Eq. (17) reduces to

$$\langle(\Delta\hat{N})^2\rangle_l = \eta_2^2\langle(\Delta\hat{N})^2\rangle + \eta_2(1-\eta_2)\langle\hat{N}\rangle, \tag{18}$$

such that

$$\Delta\phi_l^2 = \Delta\phi^2 + \frac{1-\eta_2}{\eta_2}\frac{\langle\hat{N}\rangle}{(\partial\langle\hat{N}\rangle/\partial\phi)^2}. \tag{19}$$

Thus, for the balanced case with $\phi = 0$ we find that for $|\alpha| = |\beta| = 0$

$$\Delta\phi_l^2 = \frac{1+\eta_2}{2\eta_2}\Delta\phi^2, \tag{20}$$

and for $|\alpha|,|\beta| \neq 0$

$$\Delta\phi_l^2 = \frac{1}{\eta_2}\Delta\phi^2. \tag{21}$$

As we can see from these results the effect of the detector efficiency is to reduce the sensitivity by introducing an overall prefactor. It does not change the functional form, however, thus making it possible to maintain the $1/n^2$ scaling for the uncertainty characteristic of the HL. Thus, this type of interferometer is robust against losses due to inefficient detection. This is consistent with previous results that have shown that the limitations in detection efficiency can be overcome by using a configuration that disentangles the states prior to performing the measurements [23,24], as is the case with the SU(1,1) interferometer when $\phi = 0$.

Next we study the effect of internal losses on the interferometer by setting $\eta_2 = 1$. We first look at the configuration with no input fields $(|\alpha| = |\beta| = 0)$. In this case we find after writing the uncertainty in terms of the number of internal or spontaneous photons that it is given by

$$\begin{aligned}\Delta\phi_l^2 = \Delta\phi^2 + \frac{1-\eta_1}{\eta_1}\bigg[&\frac{2(n_s+1)}{(1+\cos\phi)n_s(n_s+2)}\\ &+ \frac{1+(1-\eta_1)(n_s+1)}{\eta_1 n_s(n_s+2)^2\sin^2\phi}\bigg].\end{aligned} \tag{22}$$

As this result shows, the last extra noise term is out of phase with respect to the lossless case, which means that at $\phi = 0$, where the ideal result reaches the HL, this terms diverges, as shown in Fig. 3. It is possible to find a range of values ϕ for which the sensitivity can go below the classical limit even in this case; however, it will only be for a very limited range of n_s given that even for the ideal lossless case a small deviation from $\phi = 0$ [see Fig. 2(b)] makes it impossible to reach the HL. Thus, any internal loss in this configuration will practically make it impossible to reach the HL or beat the SQL. A similar

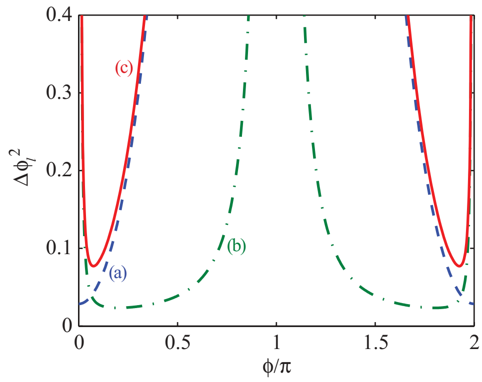

FIG. 3. (Color online) Uncertainty in the phase estimation of the SU(1,1) interferometer in the presence of internal losses for the case of no inputs, Eq. (22). The contributions from (a) the ideal lossless SU(1,1) interferometer and from (b) the extra term that results from losses are out of phase. (c) Uncertainty when the losses are taken into account. $\eta_1 = 0.9$ and $n_s = 5$.

result is obtained in the case when only one of the input ports of the interferometer is seeded with a coherent state.

Finally, we look at the configuration with coherent state inputs ($|\alpha|,|\beta| \neq 0$). As was done before, in order to simplify the results, we consider only the case where $\phi = 0$ and $\Phi = \pi/2$ in which case we find that

$$\Delta\phi_l^2 = \Delta\phi^2\left[1 + \frac{1-\eta_1}{\eta_1}(1 + 2\sinh^2 s)\right] + \frac{1-\eta_1}{\eta_1^2}\frac{1 + (1-\eta_1)(\sinh^2 s + \cosh^2 s)}{8|\alpha\beta|^2\cosh^2 s}. \quad (23)$$

If we take into account the condition in which the ideal lossless case can reach the HL ($|\alpha|^2,|\beta|^2 \gg 1$) we can neglect the contribution from the last term in the above equation, such that after writing the uncertainty in terms of n_i we find that

$$\Delta\phi_l^2 \simeq \Delta\phi^2\left[1 + \frac{1-\eta_1}{\eta_1}\frac{n_i}{|\alpha|^2 + |\beta|^2}\right]. \quad (24)$$

From this result we can see that internal losses result in an additional noise term with a prefactor that scales as n_i, such that when combined with the $1/n_i^2$ scaling for the lossless SU(1,1) interferometer it leads to a $1/n_i$ scaling for the uncertainty. Figure 4(a) shows the effect of this extra noise term due to internal losses on reaching the HL, which is given by the red dashed line. As can be seen from this figure, as long as the internal losses are less than 50% it is possible to beat the SQL, given by the red dotted line.

The extra noise term will start to dominate when its contribution is equal to the contribution of the ideal SU(1,1) interferometer, which occurs when the internal losses are

$$1 - \eta_1 = \frac{1}{1 + n_i/(|\alpha|^2 + |\beta|^2)}. \quad (25)$$

Once this happens the interferometer will not operate at the HL anymore, although it will still operate below the classical limit until the second term of Eq. (24) is significantly larger than the first one. This implies that for a given loss the interferometer will operate at the HL for a limited range of n_i. Figure 4(b) shows the amount of loss that will make the extra noise term dominate. As can be seen from this figure, even for a large interaction strength parameter s of the order of 2, an internal loss of 5% is required for the extra noise term to dominate. Therefore we can conclude that the use of coherent input states for the SU(1,1) interferometer make it robust against internal losses.

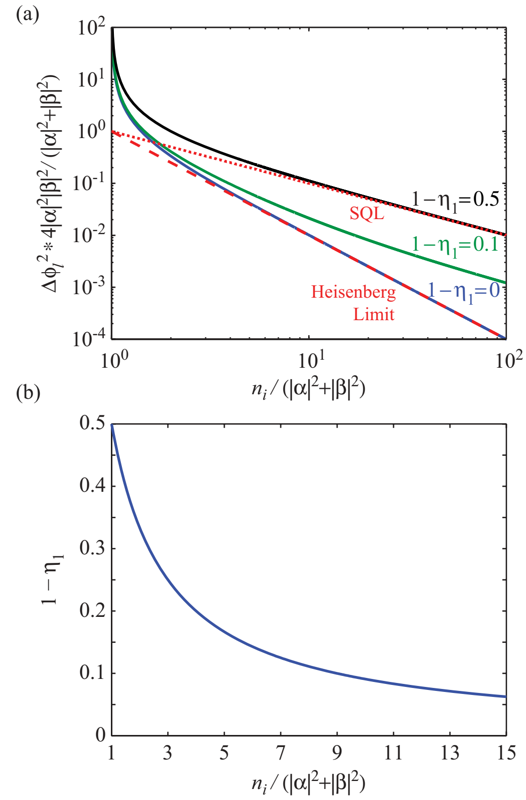

FIG. 4. (Color online) (a) Uncertainty in the phase estimation of the SU(1,1) interferometer in the presence of losses for the configuration with coherent state inputs as a function of the normalized internal number of photons, $n_i/(|\alpha|^2 + |\beta|^2)$, for different levels of internal loss $(1 - \eta_1)$. The red dashed line indicates the Heisenberg limit while the red dotted line indicates the SQL. (b) Level of loss at which the extra noise term in Eq. (24) dominates vs the normalized number of photons inside the interferometer. Note that $n_i/(|\alpha|^2 + |\beta|^2) = 15$ corresponds to $s = 1.7$.

IV. PHYSICAL IMPLEMENTATIONS

The SU(1,1) interferometer configured with input coherent states on both input ports is robust against both internal and detection losses, making this a promising configuration for an experimental implementation with current technologies. The original discussion by Yurke *et al.* [16] proposed using either parametric down-conversion or 4WM interactions for the nonlinear processes in Fig. 1. Recent work with 4WM in a double-Λ configuration in Rb vapor has led to the generation of "twin beams" with strong intensity-difference squeezing [25] and a large degree of entanglement [26]. The relatively straightforward implementation of these experiments with warm Rb vapor cells makes this 4WM configuration an ideal candidate for a possible implementation, along the lines of the implementation of this interferometer in the classical domain in Ref. [18]. There are, however, a number of experimental concerns and nonideal, or at least unexpected, behaviors that can complicate this implementation.

The twin-beam-generation experiments in the 4WM double-Λ configuration were performed by combining a relatively strong cw pump and a weak probe beam at a small angle inside a Rb cell. The atomic $\chi^{(3)}$ interaction leads to 4WM, which generates a new beam, called the conjugate, at the same angle but on the other side of the pump. In this case the system acts as a phase-insensitive amplifier. In ^{85}Rb the frequency of the probe and conjugate beams are ± 3 GHz (the ground-state hyperfine splitting) away from the pump frequency, which itself is tuned approximately 0.8 GHz from the D1 atomic resonance. Such a frequency difference is not an issue in the SU(1,1) interferometer since the photons from the two paths "interfere" with each other through the parametric process. With this process, interaction strengths as large as $s = 2$ have been demonstrated while retaining the quantum correlations that lead to intensity-difference squeezing and entanglement. This allows a large range of possible values for the internal number of photons n_i.

The simplest physical implementation of the interferometer would involve using two Rb cells to implement the two 4WM processes, with a two-lens 4f system in between the cells instead of the mirrors indicated in Fig. 1. This optical system will image the first process onto the second one, matching the spatial distribution and wavefronts of the fields in both cells. In addition, the pump, probe, and conjugate beams will be spatially separated and copropagating in the region between the two lenses, making it possible to introduce the $\pi/2$ phase shift required for the pump beam. When implementing the SU(1,1) interferometer in the configuration with both the probe and conjugate beams seeded at the input of the interferometer, the process in the first parametric region becomes phase sensitive. This makes it necessary to actively stabilize the relative phases of the input fields. The second interaction region in the interferometer is also a phase-sensitive process, which means that the beams also need to be recombined in a phase-stable manner with a pump beam that is phase-shifted by $\pi/2$ from the first interaction region. In addition, the wavefronts need to be properly mode-matched in the second cell so that this 4WM interaction can undo what the first region does. That is, if the first region generates correlated pairs of photons, they will undergo stimulated absorption in the second region.

One of the main complications with this implementation would be that the $\chi^{(3)}$ interaction also leads to a Kerr lensing (intensity-dependent index of refraction) effect due to the strong pump beam with a Gaussian profile that can distort the probe and conjugate beams [26]. The probe and conjugate beams are approximately 0.8 and 6.8 GHz away from the atomic resonance, respectively, which leads to a significantly different lensing effect for each beam. This will make the mode-matching of the two beams when recombining them in the second 4WM region more difficult, since the differential Gaussian lensing on the two beams must be compensated for. This Kerr lensing can be minimized by using a broad flat-top pump profile, but this generally requires more pump power. In addition, optical losses are somewhat hard to eliminate completely, especially if extra optics are required to improve mode-matching in the second interaction zone. Both of these effects will reduce the mode-matching efficiency in the second 4WM region and will contribute to a reduction of the sensitivity due to effective internal losses. An additional complication is due to the air currents that result from the use of hot vapor cells, because they will vary the optical path difference between the two arms of the interferometer and make stabilization of the interferometer more complicated. This, however, can be compensated for by active stabilization of the internal paths of the interferometer. Implementing the SU(1,1) interferometer using parametric down-conversion will also entail some of the same issues, to a greater or lesser degree.

Another, rather different approach to implementing the SU(1,1) interferometer is the possibility of using an atom interferometer with an interaction that can be made analogous to a 4WM interaction. Spinor Bose-Einstein condensates (BECs) can be made to interact such that, at least under some conditions, they obey a 4WM interaction Hamiltonian [27–30]. This implementation can avoid some of the complications that have been discussed above in the optical implementation.

Bose-condensed ^{23}Na in the $F = 1$ state constitutes an example of a spinor BEC. The system can be thought of as a degenerate cloud of $F = 1$ atoms with a vector order parameter. Alternatively, one can think of it as three coupled condensates, each with a different projection of spin ($m_F = 0$, $+1$, -1), population, and phase [31]. The condensates are characterized by collisional interactions as well as an interaction with an imposed magnetic field. The only important collisional interaction between the condensates is the collision of two $m_F = 0$ atoms that produces one atom in the $m_F = -1$ state and one in the $m_F = +1$ state, or vice versa. These collisions conserve the total spin projection as well as the total energy in the linear Zeeman approximation. The quadratic Zeeman energy shift is left to play off against the atom-atom interactions to determine the final distribution of the population of atoms between the three m_F states. In a Bogoliubov approximation the Hamiltonian for this system can be written as equivalent to a 4WM interaction [27].

The analogy to the optical implementation would be for most of the atoms to start in the $m_F = 0$ state, with a small population of the $m_F = \pm 1$ states. In this system the $m_F = 0$ condensate plays the role of the pump beam, while the $m_F = \pm 1$ states play the roles of the probe and conjugate beams. Applying a microwave field that is off-resonant for the $F = 1$ to $F = 2$ ground-state transition in Na, one can dress the system such that the $m_F = 0$ state is higher in energy than the $m_F = \pm 1$ states. This "turns on," or allows the collisional interactions to start generating pairs of $m_F = \pm 1$ atoms. Pairs of $m_F = \pm 1$ atoms are generated by the 4WM of matter waves in the first interaction region and then collide again to regenerate $m_F = 0$ state atoms in the second region. The microwave field can also be pulsed to give a relative phase shift between the phase of the $m_F = 0$ condensate and those of the $m_F = \pm 1$ states, allowing the phase shift between the two nonlinear interaction regions to be controlled.

In the experiments of Ref. [31] the atoms are trapped in a crossed laser dipole trap, which maintains rather stiff confinement and, under selected conditions, the atoms can be confined to a single spatial mode of the trap [32]. This confinement restricts the spatial modes of all three condensate components, enforcing essentially perfect mode-matching as long as the single-mode conditions are maintained. Similarly, beam-path stability is not an issue in this case. Losses internal to the interferometer are much less of a problem in the atomic interferometer than in the optical interferometer. Atomic losses are dominated by scattering of hot background atoms against the condensate atoms. The vacuum can be made quite good, and the lifetime of the trap can be made to be much longer (tens of seconds) than the duration of the proposed experiments (perhaps tens of milliseconds). One issue that does arise for the spinor atom interferometer is that the Hamiltonian is the exact 4WM Hamiltonian only in the Bogoliubov approximation. If the population transferred to the $m_F = \pm 1$ states becomes significant this approximation becomes invalid and the $m_F = \pm 1$ populations generated in the first region will not return to the $m_F = 0$ state in a symmetrically constructed second interaction region.

V. CONCLUSION

We have shown that the SU(1,1) interferometer can be used to reach the Heisenberg limit for the ideal lossless case for configurations with and without input fields. Both of these configurations are robust against losses that result from inefficient detectors. This type of loss only introduces a prefactor for the sensitivity but does not change its functional form. As a result, using an inefficient detector has no effect on demonstrating HL scaling with this type of interferometer. On the other hand, the effect of internal losses can be a significant limiting factor. For the configuration with no input fields (vacuum input) or only one input coherent state, any amount of internal losses will make it virtually impossible to reach the HL or even to beat the classical limit. We have shown, however, that with coherent state inputs on both ports the interferometer is robust against losses and can beat the SQL even with losses approaching 50%. The robustness of this configuration makes it a promising one for demonstrating HL scaling. In addition, we have discussed how an implementation of the SU(1,1) interferometer in an atomic system may have some real advantages over a particular optical implementation of the interferometer.

One of the main limitations of the measurement strategy for the SU(1,1) interferometer presented in this paper is its dependence on ϕ. This means that precise control of the phase difference between the two arms is required. In the future, we intend to analyze other measurement strategies to see if one exists which makes the measurement independent of the internal phase of the interferometer. For the regular Mach-Zehnder interferometer there have been recent theoretical proposals and experiments that show that such a goal is possible with the use of Bayesian parameter estimation [13,33]. Such a measurement strategy might also prove beneficial for the SU(1,1) interferometer.

ACKNOWLEDGMENT

This work was supported by the NSF (Physics Frontier Center at the Joint Quantum Institute).

[1] V. Giovannetti, S. Lloyd, and L. Maccone, Nat. Photon. **5**, 222 (2011).
[2] C. M. Caves, Phys. Rev. D **23**, 1693 (1981).
[3] R. S. Bondurant and J. H. Shapiro, Phys. Rev. D **30**, 2548 (1984).
[4] M. J. Holland and K. Burnett, Phys. Rev. Lett. **71**, 1355 (1993).
[5] O. Steuernagel and S. Scheel, J. Opt. B **6**, S66 (2004).
[6] H. Lee, P. Kok, and J. P. Dowling, J. Mod. Opt. **49**, 2325 (2002).
[7] T. Kim, O. Pfister, M. J. Holland, J. Noh, and J. L. Hall, Phys. Rev. A **57**, 4004 (1998).
[8] R. C. Pooser and O. Pfister, Phys. Rev. A **69**, 043616 (2004).
[9] M. A. Rubin and S. Kaushik, Phys. Rev. A **75**, 053805 (2007).
[10] X. Y. Chen and L. Z. Jiang, J. Phys. B **40**, 2799 (2007).
[11] G. Gilbert, M. Hamrick, and Y. S. Weinstein, J. Opt. Soc. Am. B **25**, 1336 (2008).
[12] T. Ono and H. F. Hofmann, Phys. Rev. A **81**, 033819 (2010).
[13] L. Pezze and A. Smerzi, Phys. Rev. Lett. **100**, 073601 (2008).
[14] M. Kacprowicz, R. Demkowicz-Dobrzanski, W. Wasilewski, K. Banaszek, and I. A. Walmsley, Nat. Photon. **4**, 357 (2010).
[15] G. Y. Xiang, B. L. Higgins, D. W. Berry, H. M. Wiseman, and G. J. Pryde, Nat. Photon. **5**, 43 (2011).
[16] B. Yurke, S. L. McCall, and J. R. Klauder, Phys. Rev. A **33**, 4033 (1986).
[17] W. N. Plick, J. P. Dowling, and G. S. Agarwal, New J. Phys. **12**, 083014 (2010).
[18] J. T. Jing, C. J. Liu, Z. F. Zhou, Z. Y. Ou, and W. P. Zhang, Appl. Phys. Lett. **99**, 011110 (2011).
[19] Z. Y. Ou, Phys. Rev. A **85**, 023815 (2012).
[20] U. Leonhardt, Phys. Rev. A **49**, 1231 (1994).
[21] T. Kim, Y. Ha, J. Shin, H. Kim, G. Park, K. Kim, T. G. Noh, and C. K. Hong, Phys. Rev. A **60**, 708 (1999).
[22] J. Beltran and A. Luis, Phys. Rev. A **72**, 045801 (2005).
[23] T. Kim, J. Dunningham, and K. Burnett, Phys. Rev. A **72**, 055801 (2005).
[24] J. Dunningham and T. Kim, J. Mod. Opt. **53**, 557 (2006).
[25] C. F. McCormick, A. M. Marino, V. Boyer, and P. D. Lett, Phys. Rev. A **78**, 043816 (2008).
[26] V. Boyer, A. M. Marino, R. C. Pooser, and P. D. Lett, Science **321**, 544 (2008).
[27] C. K. Law, H. Pu, and N. P. Bigelow, Phys. Rev. Lett. **81**, 5257 (1998).
[28] F. Deuretzbacher, G. Gebreyesus, O. Topic, M. Scherer, B. Lucke, W. Ertmer, J. Arlt, C. Klempt, and L. Santos, Phys. Rev. A **82**, 053608 (2010).
[29] C. Gross, T. Zibold, E. Nicklas, J. Esteve, and M. K. Oberthaler, Nature **464**, 1165 (2010).

[30] B. Lucke, M. Scherer, J. Kruse, L. Pezze, F. Deuretzbacher, P. Hyllus, O. Topic, J. Peise, W. Ertmer, J. Arlt *et al*., Science **334**, 773 (2011).

[31] A. T. Black, E. Gomez, L. D. Turner, S. Jung, and P. D. Lett, Phys. Rev. Lett. **99**, 070403 (2007).

[32] M. Scherer, B. Lucke, G. Gebreyesus, O. Topic, F. Deuretzbacher, W. Ertmer, L. Santos, J. J. Arlt, and C. Klempt, Phys. Rev. Lett. **105**, 135302 (2010).

[33] L. Pezze, A. Smerzi, G. Khoury, J. F. Hodelin, and D. Bouwmeester, Phys. Rev. Lett. **99**, 223602 (2007).